Reprint Series
8 May 1987, Volume 236, pp. 680–690

SCIENCE

Some Concepts in Reaction Dynamics

JOHN C. POLANYI

Some Concepts in Reaction Dynamics

JOHN C. POLANYI

The objective in this work has been one which I have shared with the two other 1986 Nobel lecturers in chemistry, D. R. Herschbach and Y. T. Lee, as well as with a wide group of colleagues and co-workers who have been responsible for bringing this field to its current state. That state is summarized in the title; we now have some concepts relevant to the motions of atoms and molecules in simple reactions, and some examples of the application of these concepts. We are, however, richer in vocabulary than in literature. The great epics of reaction dynamics remain to be written. I shall confine myself to some simple stories.

Experimental and Theoretical Approaches

In this section I shall discuss the experimental and theoretical tools we have used, and give an indication of their origins. Our principal experimental method has been the study of infrared (IR) chemiluminescence. The most valuable theoretical tool has been and continues to be the computer integration of the classical equations of motion. Although both of these methods belong to the modern period of reaction dynamics, both have clear antecedents in earlier times.

IR chemiluminescence derives from the presence of vibrationally excited molecules in the products of reaction. Indirect evidence for the existence of such species was obtained by M. Polanyi and co-workers in 1928 in the course of studies of the reactions of alkali metal atoms and halogens (*1*). Following a suggestion by Bates and Nicolet (*2*) and by Herzberg (*3*), McKinley, Garvin, and Boudart (*4*) looked for and found visible emission from vibrationally excited hydroxyl radicals that were formed in the reaction of atomic hydrogen with ozone. This finding was soon followed by the identification by absorption spectroscopy of vibrational excitation in the products of the reactions of atomic oxygen with NO_2 and ClO_2 (*5*).

In the same year that (*5*) appeared, we began a search (in collaboration with J. K. Cashion) for IR chemiluminescence from vibrationally excited hydrogen halides (and other hydrogen-containing compounds) that were formed in simple exchange and addition reactions. The first reaction we studied was that of atomic hydrogen with molecular halogens (*6, 7*). IR emission observed in the region from 1.5 to 4.5 μm arose from the low-pressure ($\sim 10^{-1}$ torr) room-temperature reaction

$$H + X_2 \rightarrow HX\dagger + X \qquad (1)$$

where X was Cl or Br.

At that time there was lively discussion of the possibility of a visible analogue of the maser that would operate on population-inverted electronic states (a working laser was still in the future) (*8*). Given our interests, it was natural to speculate about the properties of a vibrational laser. In our communication ("Proposal for an infrared maser dependent on vibrational excitation") (*9, 10*) we indicated a number of virtues of such a device of which I shall note two here. (i) Provided that the vibrational temperature T_V sufficiently exceeded the rotational temperature T_R (both temperatures being positive, in contrast to the negative temperatures associated with population inversion in the discussions of that date), a large number of *P*-branch transitions would exhibit population inversion (Fig. 1). We named this phenomenon "partial population inversion" and noted that lasing based on partial population inversion could ensue shortly after a thermal pulse (arising from a pulsed arc or a shock wave), since "partial cooling" would ensure that $T_V >> T_R$. (ii) A chemical reaction could be used to obtain either "partial" or "complete" population inversion. We were struck by the fact that the upper atmosphere could constitute a natural laser in the infrared that was favored by its long path length and a large number of partial population inverted transitions (*9–11*).

Vibrational lasing was first achieved by Patel and co-workers (*12*). Chemical reaction as the working process in a vibrational laser followed shortly afterward through the work of Pimentel and his associates (*13*). In both cases the major contribution to lasing came from partial population inversion, as indicated by the predominance of *P*-branch emission.

In our first communication regarding IR chemiluminescence we expressed the view that the method "promises to provide for the first time information concerning the distribution of vibrational and possibly rotational energy among the products of a three-center reaction" (*6*, p. 456). This outcome was not so readily achieved.

By 1962 it was evident that the reaction in Eq. 1, despite the fact that it had proved to be a ready source of IR chemiluminescence, converted its heat of reaction into vibration with the modest efficiency of ≤50% (*14*). This finding was met with skepticism, since it was correctly pointed out that such conversion implied that the reverse endothermic process could have so much vibration in the reagents that the reaction probability would be markedly diminished (*15*). The somewhat lame reply at that date was that "though odd, it could still be the case" (*16*, p. 279).

Today we would surmise that it is the case, since for the endothermic process $Cl + HCl \rightarrow Cl_2 + H$, a heavy particle (Cl) must approach during the brief time that the H–Cl bond remains extended; too much vibrational excitation can have the consequence that the Cl + HCl interaction is averaged over many vibrational periods, resulting in an "adiabaticity" with respect to the flow of energy into the bond about to be broken. At that time the importance of the relative timing of molecular motions (though

The author is professor of chemistry at the University of Toronto, Toronto, Canada M5S 1A1. This article is a condensed version of the lecture he delivered in Stockholm, Sweden, 8 December 1986, when he received the Nobel Prize in Chemistry, which he shared with Dudley R. Herschbach and Yuan T. Lee. It is published here with the permission of the Nobel Foundation and will also be included in the complete volume of *Les Prix Nobel en 1986* as well as in the series *Nobel Lectures* (in English) published by Elsevier Publishing Company, Amsterdam and New York. Drs. Herschbach's and Lee's lectures will appear in forthcoming issues.

recognized for other types of inelastic encounters) had not yet been documented for chemical reactions. We would later illustrate this in a computer animated film (*17*).

It was not until 1967, with the development of the methods of "measured relaxation" (MR) (*16*) and "arrested relaxation" (AR) (*18*), that the goals established 9 years earlier were truly achieved. The impediment to obtaining full quantitative data by IR chemiluminescence, or any other means, in regard to what we have termed the "detailed rate constants" $k(V',R')$ (V' is the product vibrational excitation, and R' the product rotational excitation) had been the presence of an undetermined amount of vibrational and rotational relaxation of the reaction product prior to observation.

In the MR approach (*18, 19*) this was addressed by measuring the vibrational relaxation at points along the direction of flow, and hence correcting for this effect. In the AR method (*18, 20–23*), relaxation, rather than being measured, was arrested to the fullest extent possible by the rapid removal of excited products. This was achieved by complete deactivation at a surface that was usually cooled in the range from 20 to 77 K. Arrest of relaxation yielded detailed rate constants at the level $k(V',R',T')$, where T' is the translational energy distribution in the newly formed product, obtained by subtracting the initial vibrational plus rotational distributions from the total available energy.

Concurrently with the development of these IR chemiluminescence techniques, the crossed–molecular beam method was established as a quantitative tool, particularly by Herschbach and coworkers. This method, which was the outgrowth of work in a number of laboratories, obviated problems of relaxation by conducting the reaction under single-collision conditions. Since the prime measurables were angular and translational energy distributions of the products, by 1967 a degree of overlap existed between the approaches. It was not, however, until the incorporation of universal detectors by Lee and Herschbach, following what we have come to know as the "alkali age" of beam chemistry, that the same systems could be studied by both IR chemiluminescence and molecular beam scattering.

By the time the first quantitative data began to appear, powerful theoretical tools were available that could be used to link the potential field operating between atoms A, B, and C in a reaction

$$A + BC \rightarrow AB + C \qquad (2)$$

to the motions of the particles. In the original work on the London equation (*24*) by Eyring and Polanyi (*25*) an attempt was made, in collaboration with Wigner, to solve the classical equations of motion for the reactive system A + BC. This work was taken up by Hirschfelder and Wigner (*26*), but it was not until the first computer calculations of reaction dynamics by Wall, Hiller, and Mazur (*27*) that the full power of the approach became evident.

In parallel with Blais and Bunker (*28*) our laboratory (*29*) used the approach of Wall, Hiller, and Mazur in an attempt to map out the major determinants of A + BC reaction dynamics. Both groups were inspired by the proposal made by Evans and Polanyi (*30*) over two decades earlier that vibration in a newly formed bond might originate from the release of reaction energy as the reagents approached. Detailed computation indicated that this suggestion embodied an important kernel of truth, although the full story, as might have been expected, revealed a substantially richer range of scenarios.

Energy Distribution Among Reaction Products

Experiment. In the MR method several observation windows for recording IR chemiluminescence were located along the line of streaming flow. Provided that the observation windows were situated at distances corresponding to times during which relaxation was moderate, a simple graphical extrapolation back to zero time yielded adequate values for the relative $k(v')$ (v' is the vibrational quantum number corresponding to the product vibrational energy V') (*18, 19*). Detailed numerical analyses were also made that included the effects of reaction, diffusion, flow, radiation, and collisional deactivation (*19*). A model of this sort permitted, in effect, a more intelligent extrapolation to time $t = 0$.

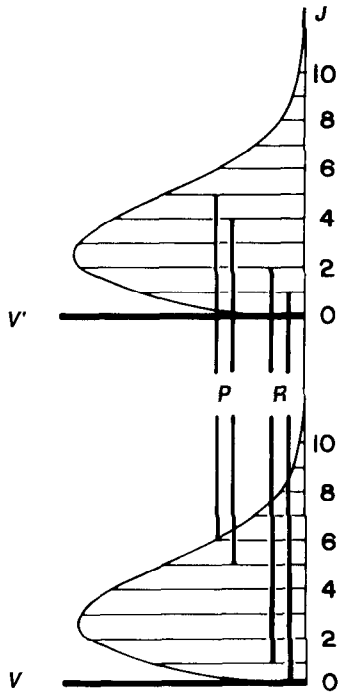

Fig. 1. "Partial population inversion." The condition $T_V >> T_R$ (>0) ensures that the population in the upper state N_u exceeds that in the optically linked lower state N_l for the indicated transitions (among others). The condition for lasing, $(N_u/g_u) > (N_l/g_l)$, where g is degeneracy, is only met for the P-branch. [Courtesy of *Applied Optics, Supplement* (*11*)]

Subsequently the flow-tube approach was applied to the determination of vibrational energy distributions in a substantial number of IR chemiluminescent reactions, particularly by Setser and coworkers (*31*) and by Kaufman and co-workers (*32*). Studies of IR chemiluminescence in flow tubes have also been extended to the elucidation of product energy distributions from ion-molecule reactions (*33*).

In the AR method two uncollimated beams of reagents met in the center of a vessel that exhibited a background pressure (with the reagents flowing) of $\sim 10^{-4}$ to 10^{-5} torr. The reaction occurred at the intersection of the beams [as demonstrated in (*20*)]. The products of reaction were transferred, after a few secondary collisions, to a deactivating surface which surrounded the reaction zone. Depending on the reagents, this surface acted as a cryopump, as a getter pump (trapping noncondensibles in excess condensible), or simply as an adsorber capable of bringing about complete vibrational deactivation (by adsorbing the product for a time sufficient to deactivate the material to its ground vibrational state $v = 0$).

The IR chemiluminescence stemming from the small fraction of molecules that emitted early in their lifetimes was collected by mirrors; this procedure increased the effective solid angle being viewed by almost a factor of 50 (*34*). By this means $\sim 10^{-9}$ torr of vibrationally excited product could be detected in one v,J (vibrotational) state.

The AR method was adopted by several laboratories, notably those of Jonathan (*35*), Setser (*36*), and McDonald (*37, 38*). It is characterized by molecular flow of the reactants and hence low densities in the reaction zone that permit observation of reaction products with highly non-Boltzmann rotational distribution as well as non-Boltzmann vibrational distributions.

The effectiveness of the combination of molecular flow plus rapid removal of reaction products in reducing relaxation to an insignificant amount in the majority of systems studied was indicated by the fact that the steady-state distribution observed under these conditions was in satisfactory agreement with the initial vibrational distribution obtained by the MR method, and that the observed rotational distribution was largely unrelaxed, indicating that collisional deactivation of vibrators, which is generally a less efficient process, was insignificant. In the case of a few very fast reactions [notably F + HBr → HF + Br (*31*)] $k(v')$ from MR were at variance with those from AR. At the low flows used in the AR instrument it appears that reaction and deactivation were occurring within the inlets, which invalidated the results (*39*); in such a case the AR rotational distributions were also found to have been relaxed (*40*).

Detailed rate constants, $k(v')$, for the reaction

$$F + H_2 \rightarrow HF + H \quad (3)$$

obtained by different procedures and by different workers over the period from 1969 to 1984 can be compared. Among the methods used was one due to Pimentel and co-workers that made use of stimulated, rather than spontaneous, IR emission (*41*). This approach was an outgrowth of the first chemical laser developed in the same laboratory (*13*). The laser approach (*41*) gave quantitative data concerning the population in the vibrational ground state $v' = 0$, which previously had been unobservable. A set of $k(v')$ values has also been obtained from crossed-molecular beam studies by Y. T. Lee and co-workers (*42*). In these demanding experiments the vibrational distribution was obtained from structure in the product translation energy distribution, which was the measured quantity. The agreement between determinations of $k(v')$ was satisfactory.

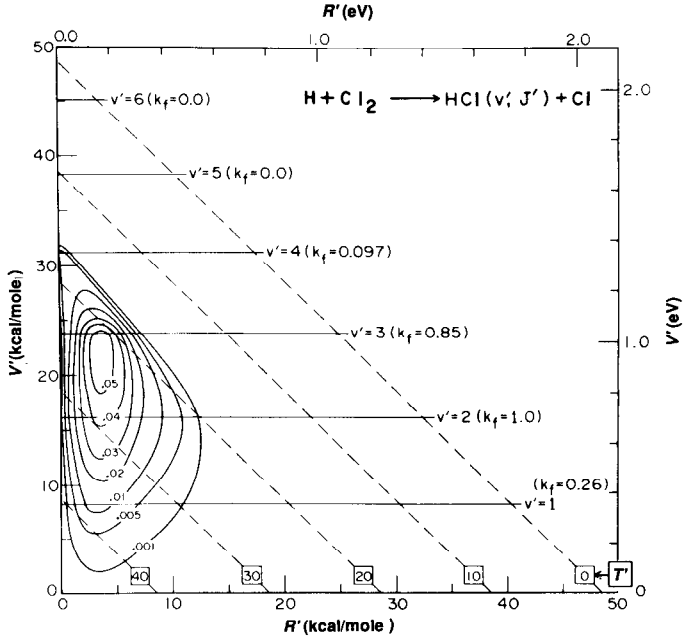

Fig. 2. Triangle plot for H + Cl_2 → HCl + Cl reaction showing the distribution of vibrational, rotational, and translational energy as contours of equal detailed rate constant $k(V',R',T')$. The ordinate is product vibrational energy, and the abscissa is the product rotational energy. Since the total available energy is approximately constant (E'_{tot} = 48.4 kcal/mole), the translational energy T', given by the broken diagonal lines, increases to 34 kcal/mole at $V' = 0$, $R' = 0$. The rate constant $k_f \equiv k(v') = \Sigma_{J'} k(v',J')$; the subscript f denotes the "forward," exothermic direction. Contours have been normalized to $k(\hat{v}') = 1.00$, where $\hat{v}'$ is the most populated vibrational level. [Courtesy of *The Journal of Chemical Physics* (*21*)]

At the time that these experiments and those described below were undertaken, quantitative data regarding $k(v')$ did not exist. The prior observation of highly vibrationally excited reaction products noted above was a qualitative finding, and left open the question of the form of $k(v')$, which could have peaked anywhere from $v' = 0$ to $v' = v'_{max}$ (the highest accessible vibrational state). In fact, the distributions observed by IR chemiluminescence were found to peak at intermediate v', so that the mean fraction of the available energy entering vibration in the new bond ranged from $\langle f'_v \rangle = 0.39$ for

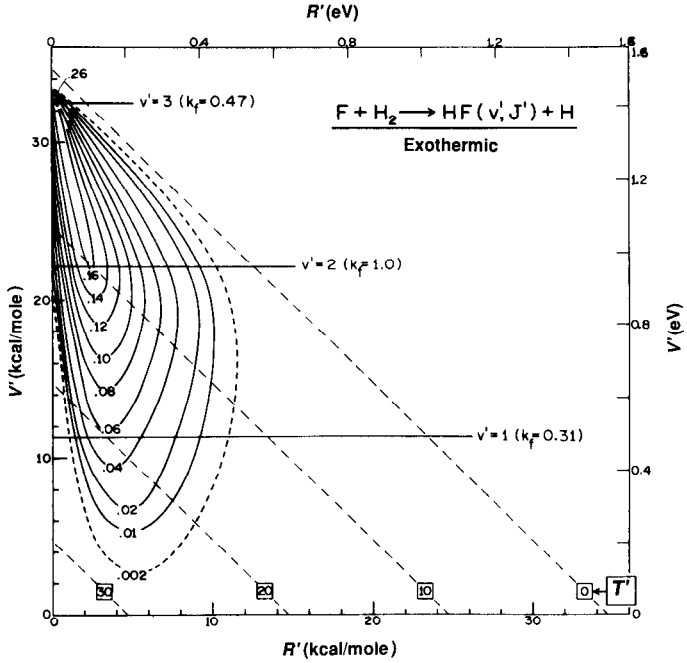

Fig. 3. Triangle plot for F + H_2 → HF + H (see caption to Fig. 6). E'_{tot} = 34.7 kcal/mole for this reaction. [Courtesy of *The Journal of Chemical Physics* (*22*)]

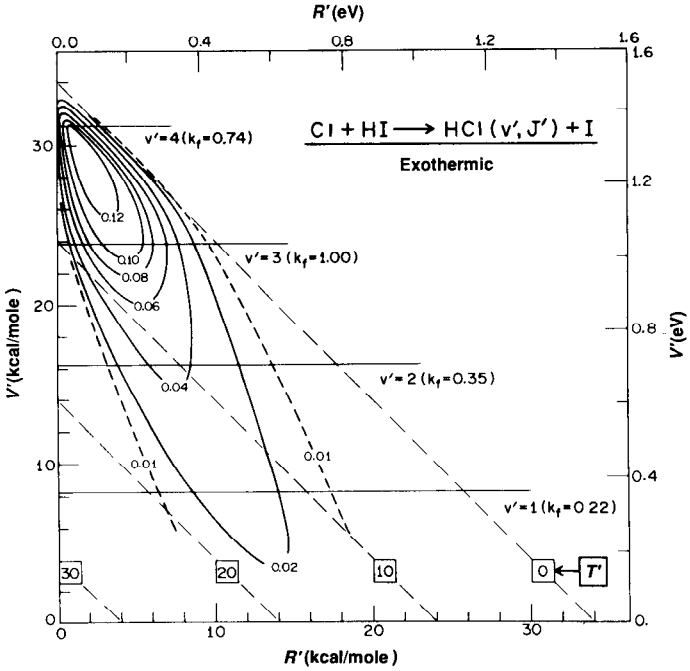

Fig. 4. Triangle plot for Cl + HI → HCl + I. See caption to Fig. 7. E'_{tot} = 34 kcal/mole. [Courtesy of *The Journal of Chemical Physics* (*20*)]

$H + Cl_2$, $\langle f'_v \rangle = 0.55$ for $H + Br_2$, $\langle f'_v \rangle = 0.53$ for $H + F_2$, $\langle f'_v \rangle = 0.66$ for $F + H_2$, and up to $\langle f'_v \rangle = 0.71$ for Cl + HI and $\langle f'_v \rangle \approx 0.9$ for $H + O_3 \rightarrow OH + O_2$.

Three examples of the graphs that we have used [as a supplement to the tabulation of the actual $k(v',J')$ values] as an aid to the visualization of the experimentally determined product energy distributions are shown in Figs. 2 through 4. By interpolation between permitted combinations of V', R', and T', we obtain contours of equal $k(V',R',T')$. In these "triangle plots," contours are shown in V',R',T' space. They delineate a "hill" of detailed rate constant in that space. Portions of the hill that lie between vibrational energy states are merely included to guide the eye as to the breadth and shape of the product energy distribution over the axis corresponding to V', R', and T'. Since classical mechanics is widely used to interpret energy distributions, these classical "fingerprints" of differing chemical reactions help us to picture contrasting types of behavior.

It is readily apparent that the first reaction, $H + Cl_2$ (Fig. 2), exhibits inefficient vibrational and rotational excitation and consequently efficient translational excitation. The second reaction, $F + H_2$ (Fig. 3), gives rise to highly efficient vibrational excitation together with inefficient rotational excitation. The third reaction pictured, Cl + HI (Fig. 4), combines efficient vibrational excitation with exceptionally efficient rotational excitation. In concurrent work alluded to in the following section, we linked these changes in dynamics to the release of repulsive energy in systems that have differing mass combination and preferred geometries of the intermediate.

The ridge of the "detailed rate constant hill" is almost vertical in the case of the first two reactions, moving out to higher R' at lower V' in the third of the reactions pictured (Cl + HI). Successively lower vibrational states therefore exhibit marked increases in translational energy in the first two cases, but a somewhat overlapped "translational energy spectrum" in the third case. This finding was seen to have interesting implications for the crossed-molecular beam chemistry, in which T' is the prime measurable. Figure 5 gives sample distributions over f'_T [blending rotational states into a continuum, since they cannot be resolved in molecular beam time-

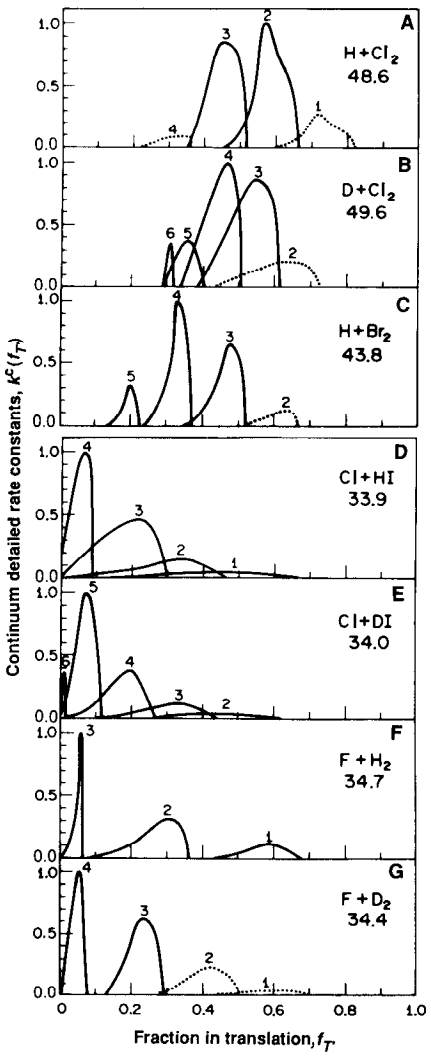

Fig. 5. Translational energy distribution in the products of some exchange reactions A + BC → AB + C obtained by subtracting the vibrational excitation measured by IR chemiluminescence from the total product energies (indicated in the figure). The vibrational states that contribute to the translational peaks are recorded above each peak. [Courtesy of *The Journal of Chemical Physics* (*45*)]

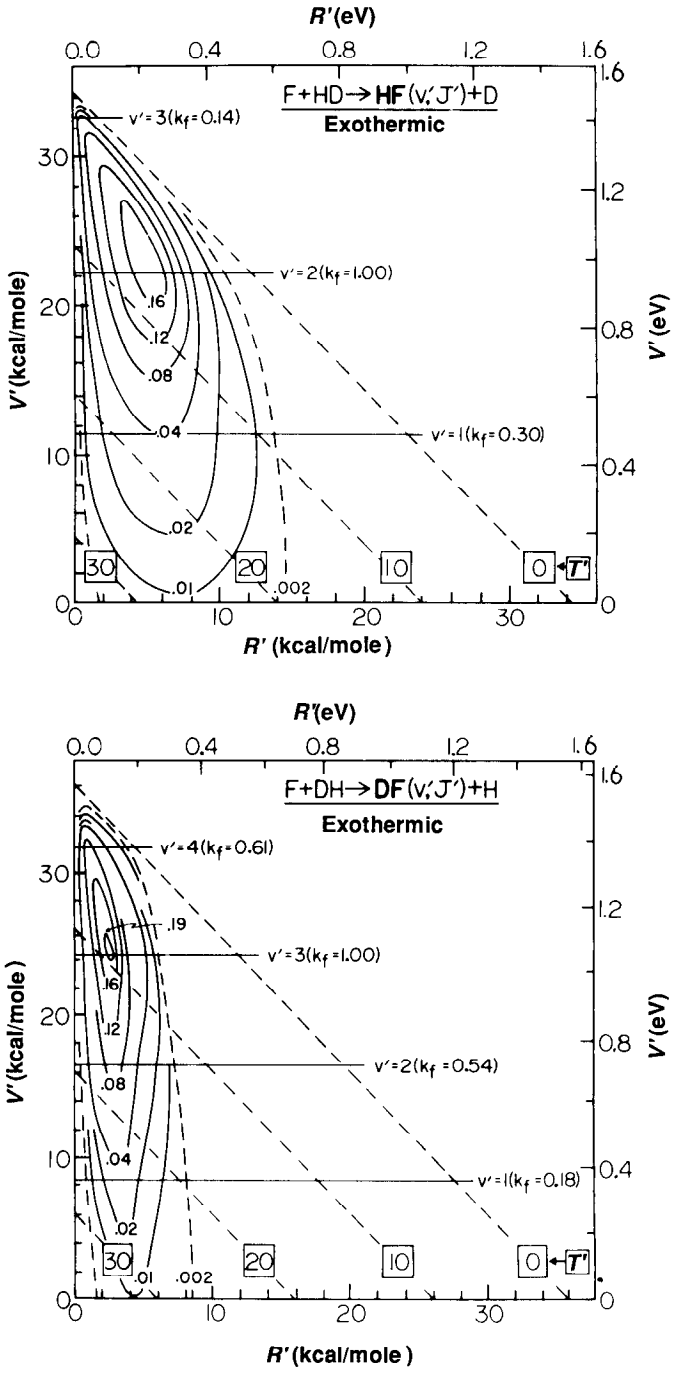

Fig. 6. Triangle plots for both branches of the F + HD exchange reaction. The total available energy in the products was taken to be $E'_{tot} = 34.3$ kcal/mole for the HF product, and $E'_{tot} = 36.1$ kcal/mole for DF, in calculating product translation T'. [Courtesy of *Chemical Physics* (*44*)]

of-flight (TOF) studies]. In the case of the F + H_2 reaction and its isotopic analogues, in addition to resolving these peaks by TOF, Y. T. Lee and co-workers have recently fully characterized the angular distribution of each (*42*).

The triangle plots, exemplified in Figs. 2 through 4, constitute one way of "compacting" the substantial data embodied in $k(v',J',T')$. The information-theory approach pioneered by Bernstein and Levine (*43*) has provided a widely used alternative method of compaction in terms of parameters that describe the deviation of the observed vibrational and rotational distributions from a statistical outcome.

Figure 6 contrasts the triangle plots for HF (Fig. 6A) and DF (Fig. 6B) formed in the thermal reaction F + HD → HF(v',J') or DF(v',J') (+ D or + H) (*44*). The forces operating are very similar but clearly are substantially more effective in rotationally exciting HF (mean fraction of the available energy entering rotation is $\langle f'_R \rangle = 0.125$) than DF ($\langle f'_R \rangle = 0.066$). This will be discussed in the section below dealing with theory.

Figure 7 shows the dramatic influence that atom C can have on the dynamics of a reaction A + BC → AB + C. Superficially the reaction illustrated resembles H + ClY → HCl + Y, for which the detailed rate constant $k(V',R',T')$ is given in Fig. 2; the difference is that the second halogen atom Y has been changed from Y = Cl to Y = I, the effect on $k(V',R',T')$ is shown. Bimodal product energy distributions were also observed in a number of other studies (*45–51*) and were regarded as indicative of the existence of two types of reaction dynamics leading to the identical product (HCl in the case illustrated). This phenomenon was termed "microscopic" branching, to distinguish it from the "macroscopic" branching that leads to chemically different products (see, for example, Fig. 6). These two types of branching are linked.

Theory. Figure 8 shows three potential-energy surfaces (PESs), all of a modified London, Eyring, Polanyi, and Sato (LEPS) variety (*29, 52, 53*), selected from a wider group examined in (*53*). The energy released as the reagents approached (termed the attractive energy release, and defined as $\mathcal{A}_\perp$ or $\mathcal{A}_T$ (*47, 48*); see the caption of Fig. 8) increases as one moves upward in the figure. In related families of reaction there is a concurrent diminution in the height of the energy barrier, and a shift of the barrier to earlier locations along the coordinate of approach with increased $\mathcal{A}$. It has proved possible to give an empirical expression to these correlations (*55, 56*).

It was found that for a substantial group of PESs (*53*) moderate percentages of energy release along the coordinate of approach (% $\mathcal{A}_\perp$) were converted quantitatively into product vibration for the **L+HH** reagent mass combination. For reactions with high % $\mathcal{A}_\perp$ the reactions moved into a new regime in which product vibration decreased with increased attractive energy release. Examination of the trajectories indicated that a transition had occurred from predominantly direct reaction [reactions in which the products, once they start to separate, continue to do so (*57*)] to indirect reaction [in which subsequent "clutching" and "clouting" secondary encounters drain the incipient vibration out of the new bond into rotation and translation (*58, 59*)]. What we were seeing was the onset of statistical behavior, in the limit of which product vibration would receive no more than its modest equipartition allocation.

At the end of the scale in which repulsive energy release predominated, low vibrational excitation was by no means the general rule; the observed vibrational excitation was strongly dependent on the

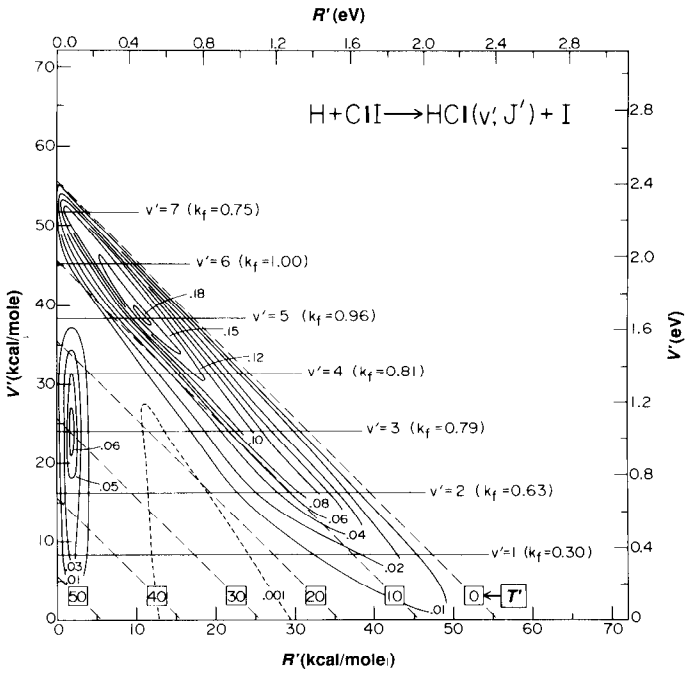

Fig. 7. Triangle plot for the reaction H + ClI at 300 K showing bimodality (18% of the HCl is in the low-J' mode, 82% in the high-J' mode). [Courtesy of *Chemical Physics Letters* (*47*)]

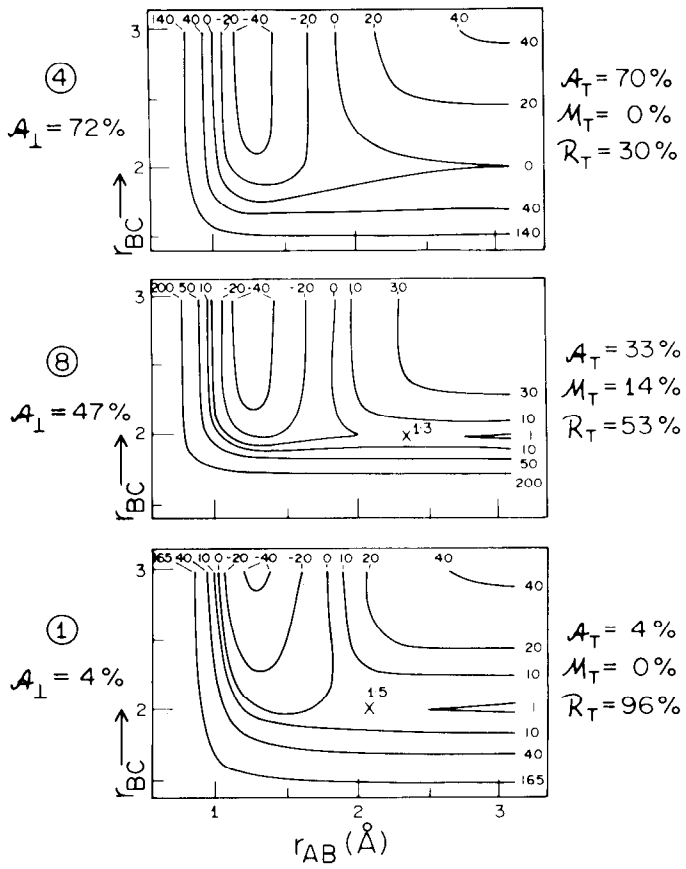

Fig. 8. Three PESs that illustrate changes in potential energy as reagents A + BC (lower right) pass through collinear transition states A--B--C to form products AB + C (upper left). Contour energies are in kilocalories per mole; all three reactions have the same exothermicity. The PESs, designated 1, 8, and 4, are arranged vertically in order of increasing "attractiveness." The PESs are indexed at the left according to the percentage attractive energy release taken from a perpendicular path across the surface ($A_\perp$ = 4, 47, and 72% for surfaces 1, 8, and 4). The same PESs are described at the right according to the percentages attractive, mixed, and repulsive energy release $\mathcal{A}_\perp$, $\mathcal{M}_T$, and $\mathcal{R}_T$ along a single collinear trajectory; this designation depends on mass combination, which was **L+HH** (**L** has a mass of 1 amu, and **H** has a mass of 80 amu). The barrier crest, designated **x**, shifts to "earlier" locations along r_{AB} as the surfaces become more attractive. [Courtesy of *The Journal of Chemical Physics* (*53*)]